Mechatronics 25 (2015) 55–64

Contents lists available at ScienceDirect

Mechatronics

journal homepage: www.elsevier.com/locate/mechatronics

Design and implementation of FPGA-based Taguchi-chaos-PSO sun tracking systems

Jui-Ho Chen, Her-Terng Yau *, Tzu-Hsiang Hung

Department of Electrical Engineering, National Chin-Yi University of Technology, Taichung 41170, Taiwan

ARTICLE INFO

Article history:
Received 4 December 2013
Accepted 23 December 2014
Available online 13 January 2015

Keywords:
Dual-axis sun tracking
INC MPPT
Fuzzy
PSO
Taguchi

ABSTRACT

The field-programmable gate array (FPGA) based intelligent sun tracking system proposed in this paper uses an NI 9642 controller to integrate the dual-axis sun tracking system with a Maximum Power Point Tracker (MPPT), so as to effectively increase the output power of solar panels. Furthermore, it is provided with multiple intelligent functions, so that the system can start up the sun tracking function automatically in the daytime, and automatically return to its initial position at night. It has a delay function to reduce the electric power consumed by the motor in rotation. Moreover, it can be switched to dual-axis or one-axis sun tracking freely as required by the user, and the solar panel inclination can be operated directly. The dual-axis sun tracking system uses the Particle Swarm Optimization (PSO) method to look for the parameters of the PI controller. The Taguchi Method and Logistic Map are proposed to enhance the steady state convergence of PSO in seeking the optimal solution. The MPPT uses Fuzzy Logic to adjust the step length of the incremental conductance method, so as to remedy the defects in the traditional fixed step method, and to make the solar panel output reach the maximum power point position rapidly and stably.

1. Introduction

In recent years, the demand for energy has been increasing; thus, more attention is being paid to energy security and environmental impact. Renewable energy sources, including wind electric power generation and solar power generation, have also received increasing attention. Among these renewable energy sources, solar power generation can generate electric power with solar irradiation, and it is noise free, requires minimal maintenance, and has no regional effect. A high intensity of sunlight irradiating on the solar panel for an extended period of time can cause the solar panel to generate more power. However, the migration of the sun and changes in the weather will influence the output power of the solar panel. Many studies have discussed ways to improve the power output of solar panels. A relatively effective method is to use MPPT technology to keep the power generation of the solar panel at the maximum power point in the present climatic conditions, and to use a sun tracking system to make the solar panel receive more sunlight.

Generally speaking, for solar power generation, the solar panel is mostly fixed at a better inclination to receive the solar irradiation in the daytime. However, the sun position varies slowly with time; in other words, the sun rises in the east and sets in the west. Therefore, a fixed solar panel cannot receive direct solar irradiation in some time intervals; thus, there is a decrease in the power generated by the panel. The sun tracking systems are mostly divided into one-axis and dual-axis tracking. One-axis means the solar panel can turn to the east and west. This structure is simple, but the south–north error results in inaccurate positioning and influences the generating efficiency. Dual-axis sun tracking has an east–west axis and a south–north axis, greatly increasing the tracking accuracy. The sun tracking modes are divided into passive and active tracking. Passive sun tracking determines the sun movement track by calculation or statistics, so that the orientation and angle of the solar panel change slowly with time. This method requires long-term statistics, and the longitude and latitude of different regions are put into the calculation so as to obtain the optimal movement orientation and angle. Active sun tracking uses optical sensors to look for the sun's position. The direction of the sun is identified according to the feedback of error signals measured by sensors, and then the solar panel is turned towards the sun [1–3].

Among the studies of sun tracking systems, in 2010, Al Nabulsi et al. proposed the 150 W photovoltaic system efficiency optimization method, using dual-axis sun tracking and MPPT [4]. The direction of the solar panel was changed by calculating the azimuth

* Corresponding author.
E-mail address: pan1012@ms52.hinet.net (H.-T. Yau).

http://dx.doi.org/10.1016/j.mechatronics.2014.12.004
0957-4158/

and elevation of the sun, and the motor was controlled by a PI controller. Finally, the perturbation and observation method was used for MPPT. In 2011, Seme et al. proposed the most efficient dual-axis sun tracking system [5], which calculates the inclination and azimuth of the sun, and uses a two-axis sun tracking system to track the sun movement track, so that the solar panel obtains the most solar illumination. In 2011, Colli et al. tested three solar panels using different forms of crystalline silicon at a solar power plant in the Italian Alps for two months, and proposed the maximum power verification method for solar panels in 2012. The method was applied to the bracket and one-axis sun tracking systems [6]. It was proved that the one-axis system could obtain more solar illumination than the bracket system, and the test in April showed that the solar panel output of the one-axis system was higher than that of the bracket system by 19%. In 2012, Dolara et al. proposed a one-axis tracking system performance analysis [7], whereby the system was analyzed in a specific power plant. The results showed that the system could effectively increase the output power of solar panels.

In terms of motor optimization PID controller design, Solihin et al. used PSO to look for the optimal parameters of the PID controller in 2011 [8], and used a PID controller to control the DC motor. The search results of four objective functions were compared. In 2011, Dongsheng et al. proposed a new type of PSO to look for PID parameters [9], retaining the advantages of traditional PSO. The PSO equation was put into the calculation of the average worst solution. Finally, this new type of PSO was used to look for the PID controller parameters of the DC motor. In 2011, Verma et al. proposed PDPSO to look for DC motor PID controller parameters [10]. The application program of PDPSO is almost identical with the traditional PSO, but it provides faster searching. In 2012, Altinoz et al. used chaotic PSO to look for PID parameters [11]. After one PSO search in the Logistic chaos map, the positions of particles were put in chaos to look for better positions, so as to prevent PSO from earlier convergence.

Generally, the MPPT in solar energy systems is usually a DC–DC converter between the solar panel and the load. By adjusting the duty cycle of the switching converter, the output power of the solar panels can be held in the maximum power point position. In order to precisely control the system at the maximum power point, it is necessary to use a good maximum power point tracking algorithm. The most commonly used algorithms are the perturb and observe (P&O) method and the incremental conductance (INC) method. The P&O method involves repeatedly adjusting the duty cycles. It can make the output power fall to near the maximum power point. However, this method will produce shock loss of power at this point. In the INC method, the traditional method usually uses a fixed step size to reach MPPT. By using larger steps, it can quickly reach the maximum power point. However, it will induce a vibration behaviour at the maximum power point. Conversely, the smaller steps will need more time to reach the maximum power point. Hence, it needs an intelligent algorithm to adjust the steps to obtain a better response. In this study, an intelligent fuzzy step algorithm is designed to reach this goal.

Many researchers have developed MPPT algorithms. Safari et al. used simulation and hardware to implement an incremental conductance method MPPT to directly control the work cycle of a Cuk converter [12]. Compared with the previous MPPT, the direct control eliminated the PWM controlling PI control loop. The experimental results showed that the system could still track the maximum power point accurately by using direct control. Mei et al. proposed a new type of variable step INC MPPT in 2011 [13], which could remedy the defect of the fixed step length of the incremental conductance method. The step length was changed by setting the threshold, and different threshold settings influenced the maximum power point tracking speed. In 2011, Abdelsalam et al. proposed the high performance adaptive perturbation and observation method based on power grid photovoltaic MPPT [14], improving the oscillation at the maximum power point of the traditional perturbation and observation method. The adaptive algorithm changed the perturbation value according to the change in system, so that there was no oscillation in the tracking process.

In sum, the output capacity of one-axis and dual-axis sun tracking systems is higher than that of traditional bracket systems. The sun tracking systems in the literature calculate the sun track. This method may need to readjust the inclination and azimuth of the sun in different places. Therefore, the design objective of this paper is to use an active sun tracking system, and to identify the azimuth of the sun by photosensitive element, so that the system is free from the region effect. The motor control part is the PI controller in this paper, the application of which can be found in the literature [15]. In order to more quickly determine the optimal solution for the PI controller, the Taguchi Method and Logistic Map were included in PSO to enhance the search speed and stability. Finally, the incremental conductance method MPPT is used, and the fuzzy step size adjuster is used to change the output step length. The fuzzy application can be seen in the literature [16–19]. Compared with the fixed step incremental conductance method, the fuzzy step approach can provide faster and more stable tracking speed.

2. Sun tracking system design

The main objective of the sun tracking system is to find the azimuth of the sun and to follow the movement track of the sun; therefore, the sun's track must be known before designing the system. To design the dual-axis sun tracking controller, generally speaking, the first axis of the dual-axis controller follows the moving track of the sun, and the second axis turns the solar panel towards the sun, if the movement track of the sun is sunrise (in the east) at 0°, and sunset (in the west) at 180°. The coordinates of the sun can be assumed to be (X, Y), where X represents the movement track and Y represents the deviation angle between the sun and the platform. A schematic diagram of the rotation angles of the dual-axis sun tracking system is shown in Fig. 1.

When the rotation angles of the first axis and the second axis of the sun tracking platform are designed, in order to make the solar panel track the sun accurately, the mounting positions and coincidence relation of the sensors are important. Four small solar panels of the same size are used as sensing elements, mounted on the four sides of the solar panel (east, west, south, north), and kept at a 45°

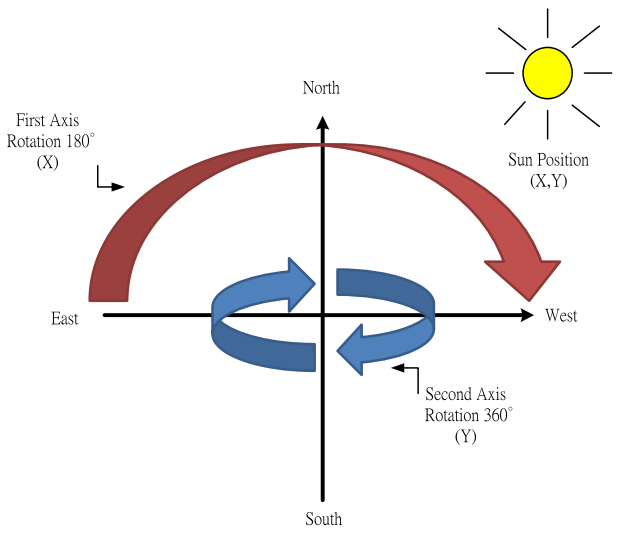

Fig. 1. Schematic diagram of platform rotation.

inclination to the solar panel, as shown in Fig. 2. The sensors are mounted in this way in order to track the sun position more efficiently. The east and west sensors of the solar panel control the first axis of the sun tracking platform, while the north and south sensors identify signals for the second axis. The sun tracking platform can identify the azimuth of the sun according to the voltage signals measured by the sensors.

The dual-axis sun tracking system is designed according to the above sun rotation angle and the sensor mounting instruction. The real sun tracking platform is shown in Fig. 3.

The solar panel mounted on the dual-axis sun tracking platform is a KC65T solar panel. The motor is an MH4013 servo motor from Taiwan Sheng Fu, the motor driver is an ADP-055-18 driver from Servo Dynamics, and the controller consists of an NI sbRIO-9642 FPGA control card and an NI 9516 motion control card for capturing the signals of the servo motor. Small solar panels are mounted on the four sides of the solar panel as sensing elements. The system structure is shown in Fig. 4.

In the servo motor control system, the transfer function of the DC motor or sync motor is shown in Fig. 5, and the AC motor can be approximated to the DC motor after magnetic field oriented control.

Where V_a is the input voltage, R_a is the armature resistance, K_T is the torque constant, I_a is the armature current, J_m is the moment of inertia, B_m is the viscous friction coefficient, K_E is the back electromotive-force constant, T_e is the motor torque, T_d is the external load, ω_m is the angular velocity and L_a is the armature inductance.

The sun tracking system controller must control the platform motor effectively to turn the solar panel to the azimuth of the sun, and it must have the following functions:

A. Manual/automatic adjustment of solar panel inclination.
B. Delay function.
C. Motor power off.
D. Automatic homing at night
E. MPPT.

This system can be switched to fixed, one-axis or dual-axis sun tracking freely according to different regions or requirements. Since the sun moves very slowly in the process of sun tracking, if the motor rotates whenever the voltage variation is sensed, it will consume too much electric power. Therefore, there must be a delay function, so that the solar panel stays for 10 min or longer before the second tracking of the sun's position in order to reduce the motor's energy consumption. Generally, the delay function is started up when the sensor error is within ±0.1 V. In this case, the delay mode may be entered due to the shielding of clouds. Therefore, the delay function in this paper is designed on dual error. When the system enters delay mode and the sensor error exceeds ±0.3 V, the system starts the second tracking. The motor power-off function means the sun movement track is fixed during dual-axis sun tracking. Therefore, when the solar panel has tracked the azimuth of the sun, power supply to the second axis motor is cut off, and is not supplied again until a deviation in the solar panel direction from the sun position is detected. The automatic homing at night means that when the sun has set and the solar illumination is very low, the solar panel returns to its original position,

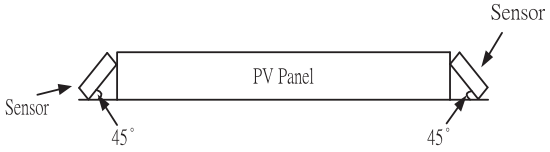

Fig. 2. Scheme of installation of sensors.

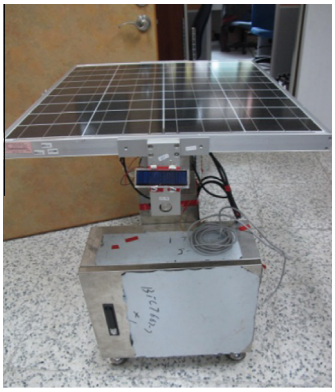

Fig. 3. Dual-axis sun tracking platform.

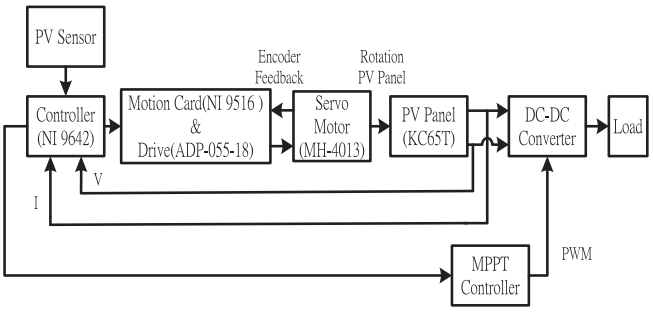

Fig. 4. Intelligent sun tracking system structure.

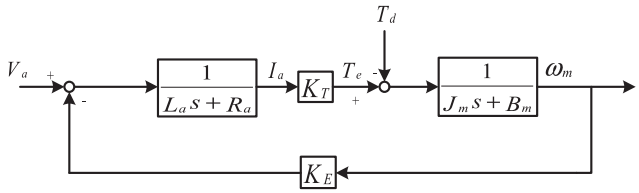

Fig. 5. Motor transfer function.

and then starts to track the sun again when the sun rises on the following day. Finally, the MPPT function means that when the sun tracking platform moves the solar panel towards the sun in delay mode, the MPPT is started up to increase the output power of the solar panel. The system control process is shown in Fig. 6.

S1, S2, S3 and S4 represent the sensors mounted on the east, west, south and north sides of the solar panel, respectively. The motor steering is controlled by identifying the error value among sensors, the motor motion is stopped and the delay time is counted till the error value is in the preset range, and the MPPT is carried out. When the delay time is up, the sun position is tracked again till the sensor error is in the preset range.

3. Optimization algorithm

In order to control the motor more efficiently, the sun tracking system in this paper uses the PI controller to control the motor. The schematic diagram is shown in Fig. 7. The PI controller is a simple structure and is likely to be implemented. This paper uses the PSO improved by the Taguchi Method and Logistic Map to work out the optimal parameter values of the PI controller. For the studies of PSO, please refer to the literature [20].

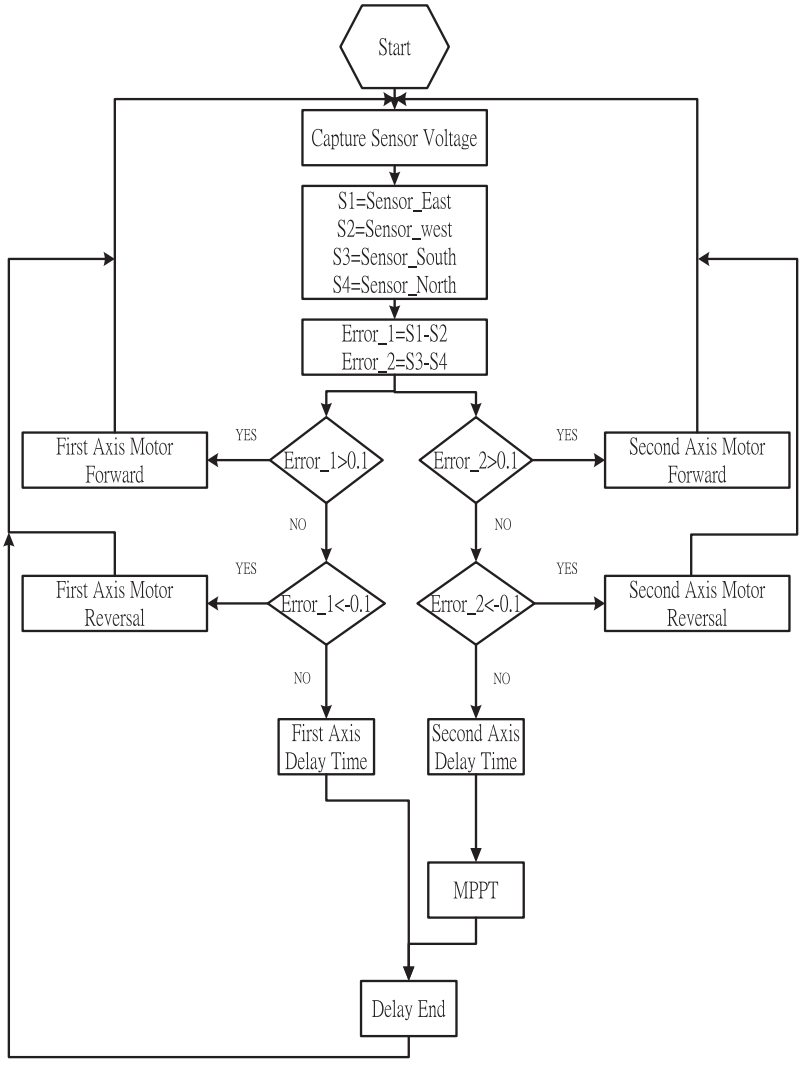

Fig. 6. Sun tracking system control flow chart.

The PI controller uses proportional gain and integral gain to calculate the controlling quantity according to the error of the system. The continuous type of error value between controller output and input can be expressed as Eq. (1), and the discrete type is expressed as Eq. (2).

$$u(t) = K_p\left[e(t) + \frac{1}{T_i}\int_0^t e(t)dt\right] \tag{1}$$

$$u(k) = K_p e(k) + K_i S(k) \tag{2}$$

where K_p is the proportional gain, T_i is the constant of integration time, $S(k)$ is the sum of the deviations, and K_I is the integral gain.

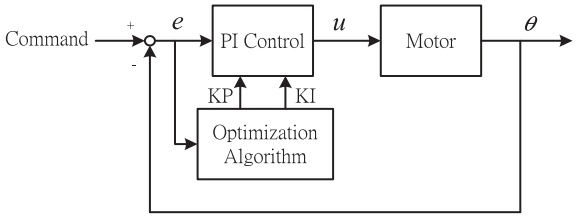

Fig. 7. Schematic diagram of motor control.

The adjustment problem of the PI controller is how to select the appropriate KP and KI parameters, so as to ensure the system has better control performance. The objective function can be defined according to our requirements. This paper uses Integrated Absolute Error (IAE) as the objective function; its mathematical definition is expressed as Eq. (3):

$$\text{IAE} = \int_0^\infty |e(\tau)|d\tau \tag{3}$$

When the objective function is defined, PSO is used to identify the optimal control parameters of the PI controller, so as to minimize the objective function. PSO was proposed by Eberhart and Kennedy, developed from observation of the foraging behaviour of birds. PSO imagines the particles as birds flying in the sky, with each particle generating an adaptive value, and Pbest and Gbest are found from these adaptive values. After each search, the position and velocity of the next search are determined by Pbest and Gbest. The optimal solution to the system can be determined by several iterative computations [21,22].

PSO determines the optimal solution of particles by several iterations. The optimal solution in each iteration can be identified, and is called Pbest. When all of the particles have been found, Gbest can be determined, and the principal factors influencing particles looking for the optimal solution are the velocity updating and

position updating of particles. The velocity updating equation is expressed as Eq. (4), and the position updating is expressed as Eq. (5). The program flow chart is shown in Fig. 8.

$$V_i(t) = W \times V_i(t-1) + C_1 \times \text{Rand} \times (\text{Pbest} - X_i) + C_2 \times \text{Rand} \times (\text{Gbest} - X_i) \quad (4)$$

where V_i is the velocity of each particle, i is the number of particles, W is the Inertia Weight, C_1 and C_2 are learning constants, Rand is a random number between 0 and 1, Pbest is the optimal solution for each particle up to now, Gbest is the optimal solution for all particles up to now, and X_i is the position of each particle.

Position updating equation:

$$X_i(t) = X_i(t-1) + V_i(t) \quad (5)$$

When PSO is used, three groups of parameters must be set, i.e., learning factors $C1$ and $C2$ and weight W. The three numerical values are adjusted under the empirical rule, which is to say, multiple adjustments are required before the numerical value suitable for the overall system is known. Therefore, the Taguchi Method is used to shorten the adjustment time. Originally, there should be 27 tests conducted in order to know which group of parameters could have a better result, whereas by using the orthogonal array of the Taguchi Method, the best result can be obtained by only nine tests. Table 1 is the $L_9(3^3)$ orthogonal array.

The Taguchi Method is applied to management and cost calculation, so the best value is calculated by S/N ratio. This paper uses the Taguchi Method to identify the three parameters, which could be adjusted for PSO. The system objective function is IAE, so the S/N ratio uses IAE directly to calculate the result. The three parameters are put in the PSO program according to the orthogonal array order, and the IAE value obtained at each time is recorded. After nine computations, the best values are calculated by Table 2, the $C1$ optimal solution is 0.5, the $C2$ optimal solution is 1.5, and the W optimal solution is 0.9.

Table 1
$L_9(3^3)$ orthogonal array.

Number of test	$C1$	$C2$	W	IAE
1	0.5	0.5	0.9	63.89
2	0.5	1	0.6	80.66
3	0.5	1.5	0.3	64.43
4	1	0.5	0.6	69.88
5	1	1	0.3	98.33
6	1	1.5	0.9	63.72
7	1.5	0.5	0.3	146.89
8	1.5	1	0.9	64.03
9	1.5	1.5	0.6	63.94

When the three unknown parameters of PSO are adjusted by the Taguchi Method, the Rand function in the velocity updating equation of PSO is a random number between 0 and 1. Therefore, the numerical values generated by each implementation of the program are different, influencing the **steady state convergence** of PSO in looking for the optimal solution. This influence is not likely to be strong, but as the complexity of the system increases, obvious differences will be felt. In order to enhance the stability of PSO in looking for optimal parameters, this paper uses Logistic to replace the Rand function in PSO velocity updating.

Chaos is a type of nonlinearity, seemingly disorderly, but regular to some extent. Logistic Map is an extensively used chaos; its mathematical expression is Eq. (6).

$$X(n+1) = r \times X(n) \times (1 - X(n)) \quad (6)$$

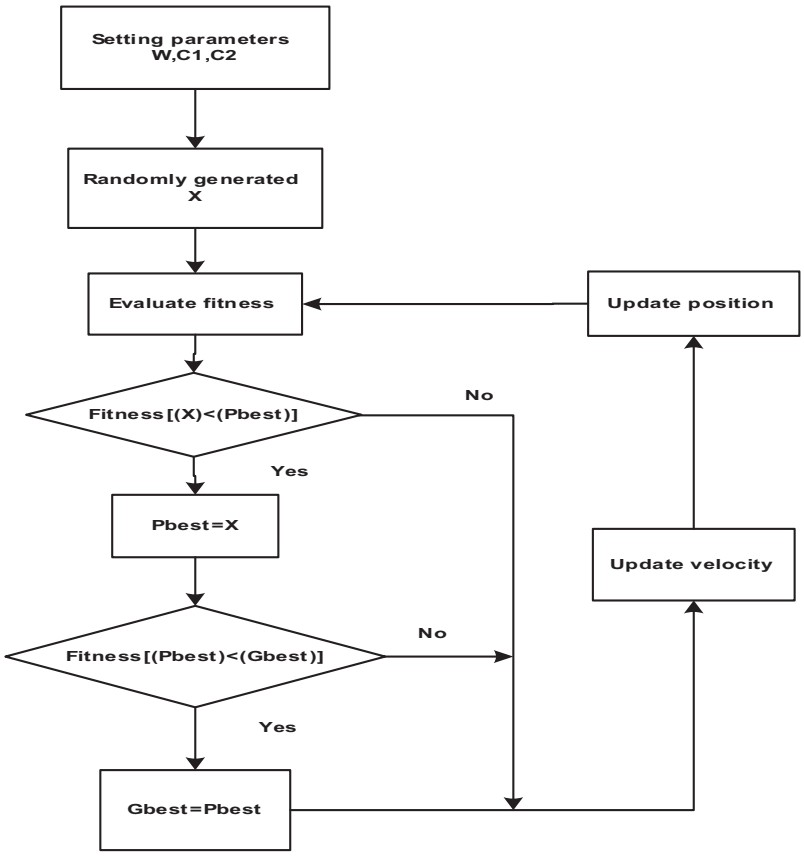

Fig. 8. PSO flow chart.

Table 2
Optimal parameter calculation.

	C1	C2	W
Level 1	208.98	280.66	191.64
Level 2	231.93	243.02	214.48
Level 3	273.97	192.03	309.65

where the range of r is 0–4, $X(n)$ is between 0 and 1, which is to say, when $X(n)$ is given an initial value, the next value, i.e., $X(n+1)$ can be worked out. When the r value is smaller than 2.8, a stable value can be obtained after several iterations. When r is between 3 and 3.5, two values occur repeatedly. When r is between 3.5 and 4, there will be nonrepetitive disorderly variation values, i.e., chaos. The output result is changed when the r value is changed, as shown in Fig. 9 [23,24]

It is obvious that when the r value is 4, the value generated is between 0 and 1, identical with the Rand function in PSO, and the disorder of Logistic Map is calculated by Entropy, as shown in Fig. 10. It is observed that the disorder is at its maximum when r equals 4, so the r of Logistic Map is set as 4 to replace the original Rand function.

In order to test whether the stability of PSO can be enhanced, the PI parameter of the motor controller is searched for under the same setting. The Rand function and Logistic Map are used respectively for five consecutive executions to compare **the steady state convergence** of IAE, KP and KI. Fig. 11 shows the result of the Rand function. Fig. 12 shows the result of Logistic Map. According to the KP and KI curves, the **steady state convergence** of the original Rand function is not very good, whereas Logistic Map results in a relatively stable convergence value of PSO in looking for the optimal solution.

4. MPPT

In order to keep the output of the solar panel at its maximum power point, this paper uses the MPPT algorithm of the incremental conductance method, but the step size of the traditional incremental conductance method is fixed. Therefore, the maximum power point can be reached rapidly when the step is large. However, there is oscillation in the steady state, so that the output power decreases. This oscillation is very low when a small step is used in the steady state, and the maximum power point is reached after a longer time. In order to remedy the defects in the incremental conductance method, some scholars have proposed the variable step incremental conductance method [25] to solve the problem. When the steady state is reached by using a larger step in transient, a smaller step is used to remedy the defects in the traditional incremental conductance method. Therefore, this paper uses the advantages of the variable step incremental conductance method for improvement, and uses a fuzzy step size adjuster to adjust the step size. Thus, the maximum power point can be reached faster compared with the variable step incremental conductance method.

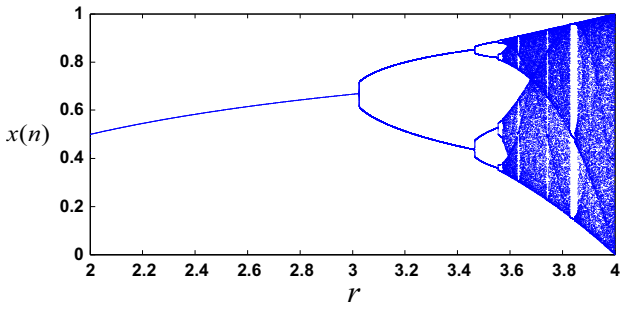

Fig. 9. Branching diagram of logistic values.

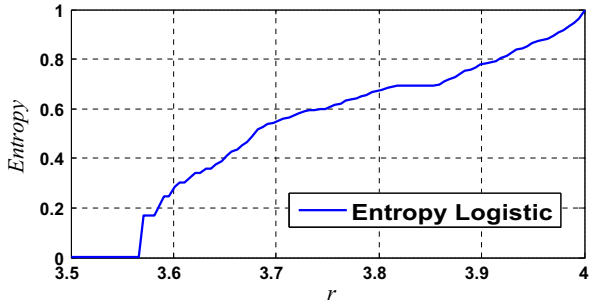

Fig. 10. Entropy of Logistic Map.

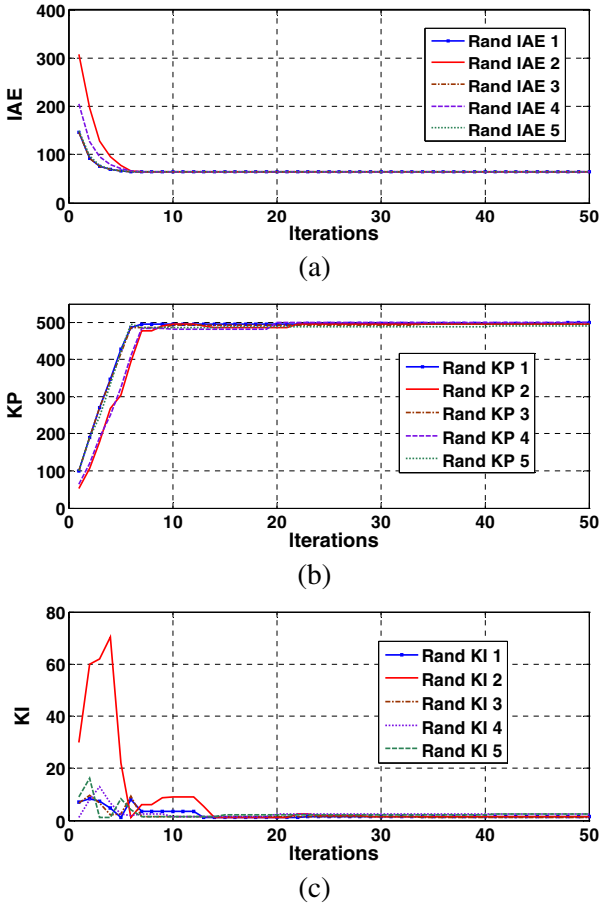

Fig. 11. Convergence curves of Rand (a) IAE, (b) KP and (c) KI.

The design of the general fuzzy step size adjuster consists of four steps: (1) define input and output variables; (2) define membership function; (3) design fuzzy rule base and fuzzy inference engine; and (4) select the Defuzzifier method [26,27]. The structure diagram is shown in Fig. 13.

In order to effectively adjust the output step size of the fuzzy step size adjuster, the power level and trend of the solar panel must be identified. Therefore, the fuzzy step size adjuster input end is dP/dV and the solar panel output power is P; dP is the power variation rate, and dV is the voltage change rate. The present trend of power is obtained from the variation rate, so as to adjust the output step size, and the accuracy rate of step size change can be increased by

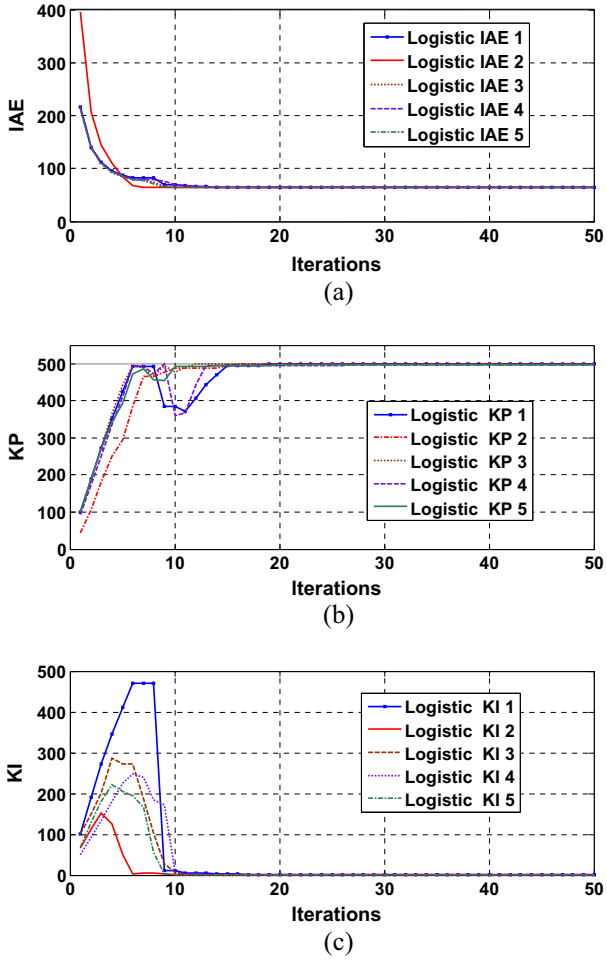

Fig. 12. Convergence curves of Logistic (a) IAE, (b) KP and (c) KI.

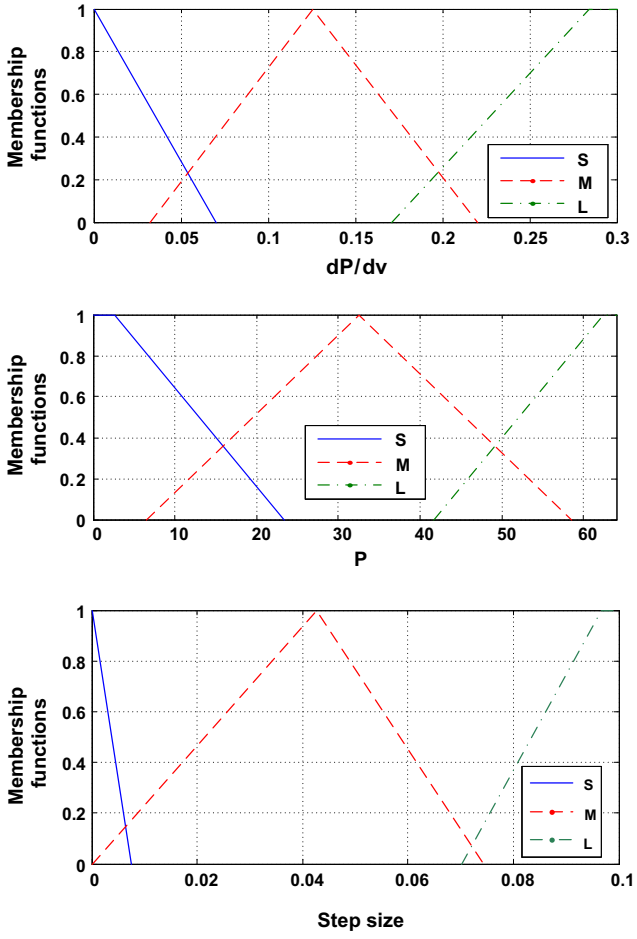

Fig. 14. Input and output membership functions.

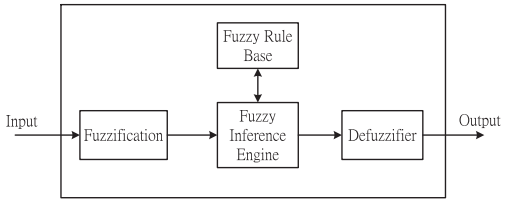

Fig. 13. Fuzzy step size adjuster structure.

Table 3
Fuzzy rule base.

		P		
		L	M	S
dP/*dV*	L	S	L	L
	M	S	M	L
	S	S	S	M

identifying the present output power. Therefore, the fuzzy step size adjuster has two input variables and one output variable, converted into a membership function by the corresponding fuzzy set, as shown in Fig. 14. The range of input variable *dP*/*dV* is [0,0.3], the power range is [0,64], and the output variable range is [0,0.1]. Each membership function has three functions, which are large (L), middle (M) and small (S). The range is adjusted according to the empirical rule.

The fuzzy rule base is determined according to the input and output membership functions, and there are two input variables, each of which has three membership variables, so there will be nine rules, as shown in Table 3.

5. Simulation and experimental results

To demonstrate the performance of the proposed controller, MATLAB/Simulink was used for simulation and the field-programmable gate array (FPGA) sbRIO-9642 was chosen as the platform for low-level time-critical signal processing, feedback control and sensing tasks. sbRIO was chosen due to its rapid prototyping environment and ease of interfacing with hardware devices, sensors and actuators. It runs as a slave under Beagleboard with which it communicates using a 10/100 Mbits/s Ethernet port available on this model of sbRIO. The controller commands the motor to rotate to change the motor rotation angle. The optimal motor PI controller parameter is found by PSO, which determines the parameter values. The KP and KI parameters are 495.2416 and 2.0339 respectively, and then the parameters are put in motor control to observe the dynamic response of the motor. In order to test the motor control reverse motor response, the pulse wave signal is added in. The motor response diagram is shown in Fig. 15.

In order to verify the simulated PI parameter, the optimal parameter found by PSO is put in the actual motor control. Fig. 16 shows the actual dynamic response of the motor. It shows that a quick actual system response can be obtained by using these simulated parameters.

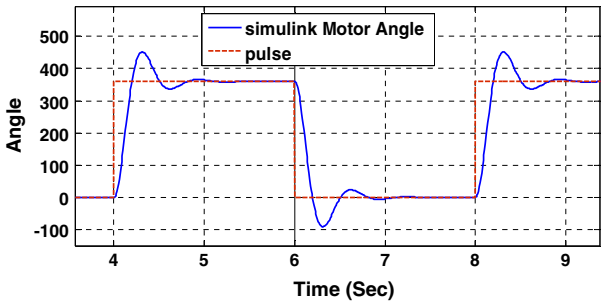

Fig. 15. Simulated dynamic response of the motor.

In terms of MPPT simulation, the power, voltage and current curve diagrams of the traditional fixed step incremental conductance method, the variable step incremental conductance method and the fuzzy step incremental conductance method are compared. The test conditions are standard test conditions (1 kW/m^2, A.M.1.5, 25 °C) for MPPT. The comparison results are shown in Fig. 17 which shows that a fixed step size method takes 0.65 s to reach the steady state, the variable step size method needs about 0.07 s and the fuzzy step method takes about 0.05 s. Therefore, it can be concluded that the fuzzy step incremental conductance method is effective in reducing the time it takes to reach the steady state.

When the intelligent sun tracking system was simulated, the dual-axis sun tracking was tested and the MPPT was started up in delay mode. The test time was 10 a.m. on May 28, 2013, and the site was the seventh floor of the Engineering Hall, National Chin-Yi University of Technology. The weather was cloudy, and the illumination was not high. Fig. 18 shows the onsite hardware architecture. The dual-axis test signals are shown in Figs. 19–23. The MPPT signal is shown in Fig. 24. It can be clearly seen that the measured errors of sensors fall within a set range and reach the MPPT at the same time after starting the tracking system. In order to show that this scheme can be applied for a longer period of time, the result for 120 min long-term sun tracking with MPPT is shown in Fig. 25. It can be seen that the control is active at t = 10 min and then the sun tracking system continues to keep on MPPT.

Finally, after the dual-axis sun tracking and MPPT test, the main point is to reduce the external power supply equipment, so that the intelligent sun tracking system can work independently. The additional electric equipment for the system consists of an **NI 9642 FPGA controller**, an NI 9516 motion card and an ADP-055-18 motor driver. Therefore, the sun tracking system is powered by a lead-acid battery. The DC/DC converter supplies power to the sun tracking system. The battery operation process is shown in Fig. 26. The electric power generated by the solar panel is not supplied to the sun tracking system directly, because it is influenced by the illumination, and thus the voltage is likely to be unstable. The sun tracking system fails when the illumination is too low, so the lead-acid battery is used as an auxiliary power supply to supply stable power.

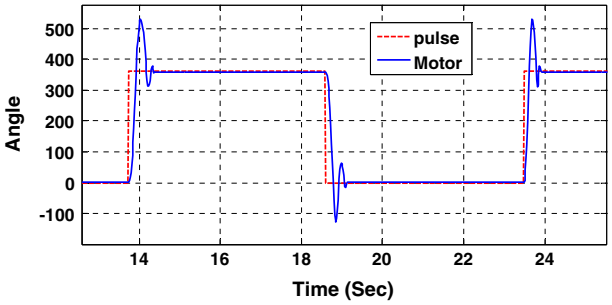

Fig. 16. Actual dynamic response of the motor.

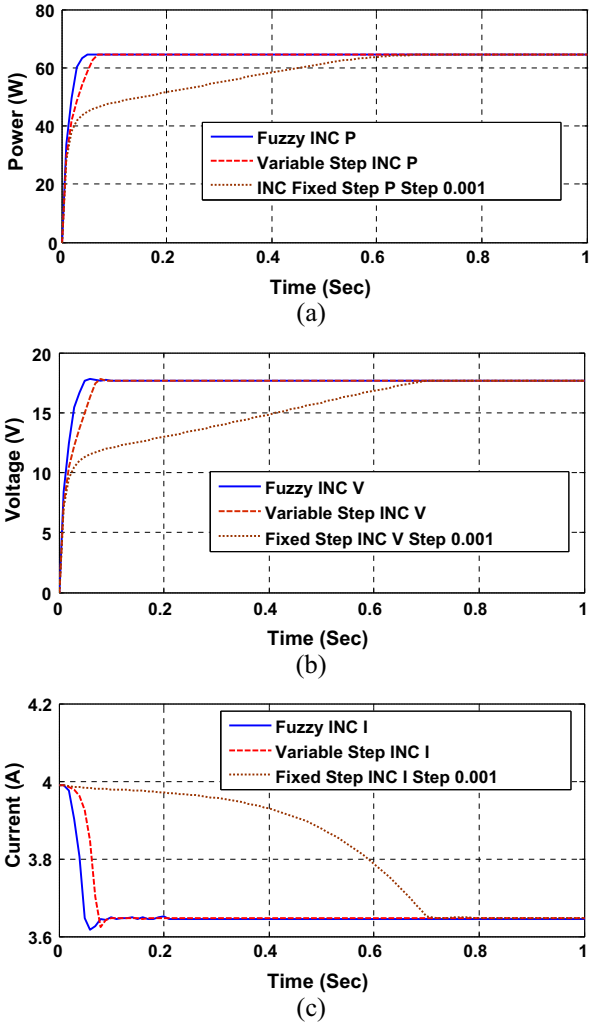

Fig. 17. Comparison of three incremental conductance methods: (a) power, (b) voltage and (c) current.

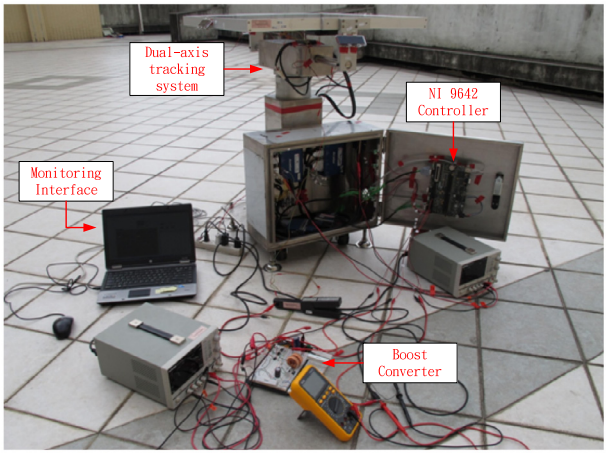

Fig. 18. Onsite hardware architecture.

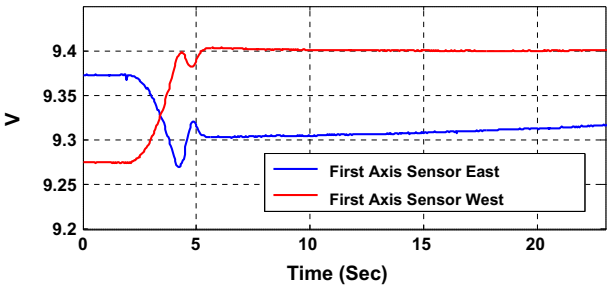

Fig. 19. Actual first axis sensor voltage.

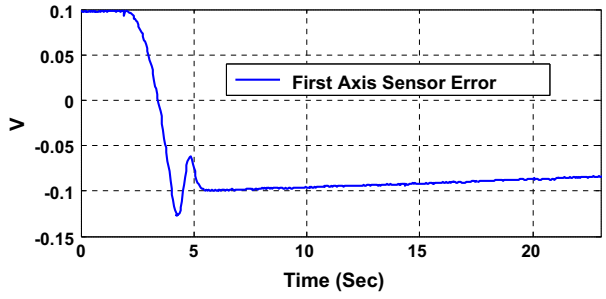

Fig. 20. Actual first axis sensor voltage error.

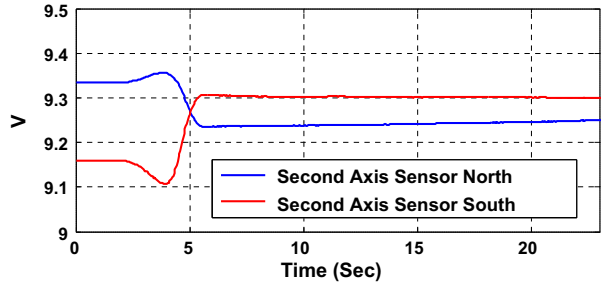

Fig. 21. Actual second axis sensor voltage.

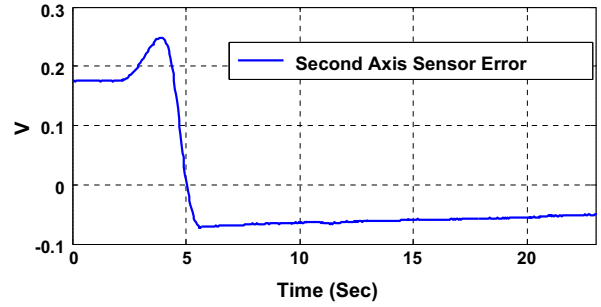

Fig. 22. Actual second axis sensor voltage error.

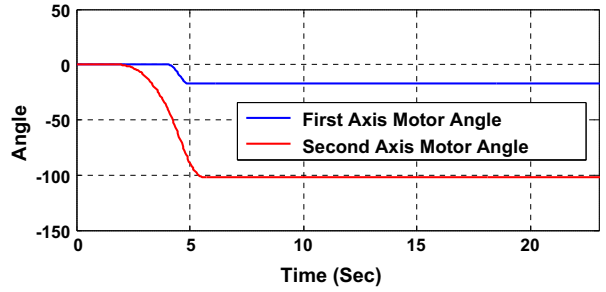

Fig. 23. Actual motor angles.

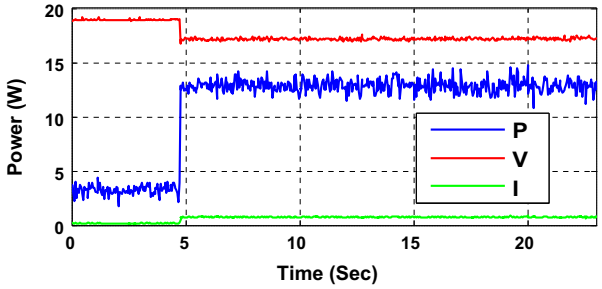

Fig. 24. Actual maximum power point curves.

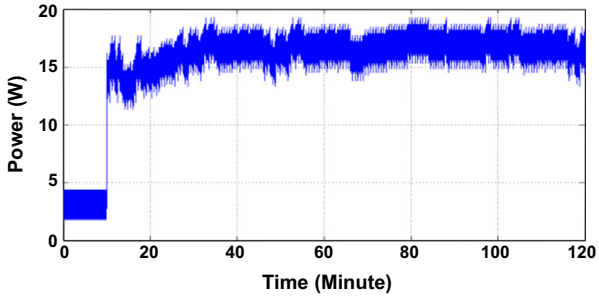

Fig. 25. Long-term sun tracking with MPPT.

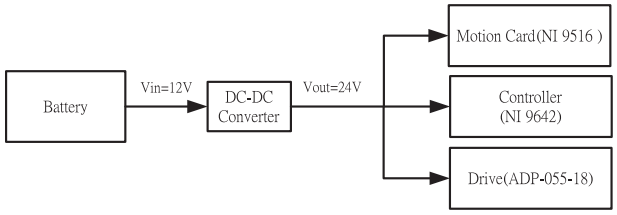

Fig. 26. Schematic diagram of the battery operation.

6. Conclusion

The intelligent sun tracking system proposed in this paper is combined with a dual-axis sun tracking system and MPPT, designed with the assistance of MATLAB, so that the system can be switched to dual-axis sun tracking, one-axis sun tracking and fixed solar panel freely according to different users and regions. In addition, the system has a delay function and a night automatic homing function to avoid the motor consuming too much electric power. For the PI controller parameter of motor control, Logistic and the Taguchi Method are used to enhance the stability of PSO in searching for the optimal solution, so as to determine the optimal parameters faster and more stably. In terms of MPPT, the fuzzy step size adjuster is used to remedy the defects in the large step or small step of the traditional incremental conductance method. The experimental results suggest that the fuzzy step size adjuster can reach the maximum power point more rapidly and stably than the traditional fixed step, and the motor dynamic response and sensor signal of the dual-axis sun tracking system are within the control range, proving that this system has multiple intelligent functions and can determine the sun position rapidly and accurately while keeping vertical to the sun. This intelligent sun tracking system may be combined with a battery management system in the future, so that it can charge and protect the battery to enhance the integrity of the system.

Acknowledgements

Financial support for this research is provided by the National Science Council of Taiwan, under the Project No. NSC- 100-2628-E-167 -002 -MY3 is greatly appreciated. The author also would like to thank Prof. Chih-Jer Lin for his valuable comments on FPGA.

References

[1] Taherbaneh M, Rezaie AH, Ghafoorifard H, Rahimi K, Menhaj MB. Maximizing output power of a solar panel via combination of sun tracking and maximum power pointtracking by fuzzy controllers. Int J Photoenergy 2010;2010. 13 pages.
[2] Roth P, Georgiev A, Boudinov H. Cheap two axis sun following device. Energy Convers Manage 2005;46:1179–92.
[3] Chin CS, Babu A, McBride W. Design, modeling and testing of a standalone single axis active solar tracker using MATLAB/Simulink. Renew Energy 2011;36:3075–90.
[4] Al Nabulsi A, El Nosh A, Ahli A, Sulaiman M, Dhaouadi R. Efficiency optimization of a 150 W PV system using dual axis tracking and MPPT. IEEE Int Energy Conf Exhib 2010:400–5.
[5] Seme S, Stumberger G, Vorsic J. Maximum efficiency trajectories of a two-axis sun tracking system determined considering tracking system consumption. IEEE Trans Power Electron 2011;26:1280–90.
[6] Colli A, Zaaiman WJ. Maximum-power-based PV performance validation method: application to single-axis tracking and fixed-Tilt c-Si systems in the Italian Alpine region. IEEE J Photovoltaics 2012;2:555–63.
[7] Dolara A, Grimaccia F, Leva S, Mussetta M, Faranda R, Gualdoni M. Performance analysis of a single-axis tracking PV system. IEEE J Photovoltaics 2012;2:524–31.
[8] Solihin MI, Tack LF, Kean ML. Tuning of PID controller using particle swarm optimization (PSO). Int Conf Adv Sci 2011;1:458–61.
[9] Dongsheng Wu, Qing Yang, Dazhi Wang. A novel PSO-PID controller application to bar rolling process. Control Conf (CCC) 2011:2036–9.
[10] Verma HK, Jain MC. A performance-dependent PSO based optimization of PID controller for DC motor. Int Conf Electr Energy Syst 2011:198–202.
[11] Altinoz O Tolga, Yilmaz A Egemen, Weber G Wilhelms. Application of chaos embedded PSO for PID parameter tuning. Int J Comput Commun 2012;7:204–17.
[12] Safari A, Mekhilef S. Simulation and hardware implementation of incremental conductance MPPT with direct control method using Cuk converter. IEEE Trans Ind Electron 2011;58:1154–61.
[13] Mei Q, Shan M, Liu L, Guerrero JM. A novel improved variable step-size a novel improved variable step-size method for PV systems. IEEE Trans Ind Electron 2011;58:2427–34.
[14] Abdelsalam AK, Massoud AM, Ahmed S, Enjeti P. High-performance adaptive perturb and observe MPPT technique for photovoltaic-based microgrids. IEEE Trans Power Electron 2011;26:1010–21.
[15] Yau HT, Hung TH, Hsieh CC. Bluetooth based chaos synchronization using particle swarm optimization and Its applications to image encryption. Sensors 2012;12:7468–84.
[16] Yörükoğlu A, Altuğ E. Estimation of unbalanced loads in washing machines using fuzzy neural networks. IEEE Trans Mech 2013;18:1182–90.
[17] Ho TH, Ahn KK. Speed control of a hydraulic pressure coupling drive using an adaptive fuzzy sliding-mode control. IEEE Trans Mech 2012;17:976–86.
[18] Li Y, Cai C, Lee KM, Teng F. A novel cascade temperature control system for a high-speed heat-airflow wind tunnel. IEEE Trans Mech 2013;18:1310–9.
[19] Tanaka K, Tanaka M, Ohtake H, Wang HO. Shared nonlinear control in wireless-based remote stabilization: a theoretical approach. IEEE/ASME Trans Mech 2012;17:443–53.
[20] Lin CJ, Yau HT, Tian YC. Identification and compensation of nonlinear friction characteristics and precision control for a linear motor stage. IEEE Trans Mech 2013;18:1385–96.
[21] Eberhart R, Kennedy J. A new optimizer using particle swarm theory. Proc Sixth Int Symp Micro Mach Hum Sci 1995:39–43.
[22] Robinson J, Rahmat-Samii Y. Particle swarm optimization in electromagnetics. IEEE Trans Antennas Propag 2004;52:397–407.
[23] Parthasarathy S, Güemez J. Synchronisation of chaotic metapopulations in a cascade of coupled logistic map models. Ecol Modell 1998;106:17–25.
[24] Alun Lloyd L. The coupled logistic map: a simple model for the effects of spatial heterogeneity on population dynamics. J Theor Biol 1995;173:217–30.
[25] Liu F, Duan S, Liu F, Liu B, Kang Y. A variable step size INC MPPT method for PV systems. IEEE Trans Ind Electron 2008;55:2622–8.
[26] Raju GVS, Zhou J. Adaptive hierarchical fuzzy controller. IEEE Trans Syst, Man Cybern 1993;23:973–80.
[27] Wu ZQ, Mizumoto M. PID type fuzzy controller and parameters adaptive method. Fuzzy Sets Syst 1996;78:23–35.